Emissions of climate-altering species from open vegetation fires in the Mediterranean region

Rabia Ali Hundal[1,2,3], Saurabh Annadate[1,2,3], Rita Cesari,[4] Alessio Collalti[5,6] , Michela Maione[1,2], Paolo Cristofanelli[1,]*

[1] Institute of Atmospheric Sciences and Climate (ISAC), National Research Council, 73100, I-40129 Bologna, Italy

[2] University of Urbino - Department of Pure and Applied Sciences, I-61029, Urbino, Italy

[3] Scuola Universitaria Superiore Pavia (IUSS), I-27100, Pavia, Italy

[4] Institute of Atmospheric Sciences and Climate (ISAC), National Research Council, 73100, Lecce, Italy

[5] Forest Modelling Lab., Institute for Agriculture and Forestry Systems in the Mediterranean (ISAFOM), National Research Council of Italy, 06128, Perugia, Italy

[6]National Biodiversity Future Center (NBFC), 90133, Palermo, Italy

**Corresponding author: Paolo Cristofanelli, phone: +39 051 6399597, fax: +39 051 6399658, p.cristofanelli@isac.cnr.it*

Abstract

The observed and projected climate change over the Mediterranean region poses serious concerns about the role of open vegetation fires (OVFs) in the emissions of climate-altering species. The aim of this study is dual. First, to review existing methodologies to quantify the greenhouse gases (GHGs) and black carbon (BC) emissions from OVFs. Then, by using four state-of-the-art emission inventories, to provide an assessment of the Mediterranean region as a source of carbon dioxide (CO_2), methane (CH_4), nitrous dioxide (N_2O), and black carbon (BC) for the period 2003-2020.

Our analysis revealed discrepancies among the four analyzed inventories (GFEDv4.1s, GFASv1.2, FINN 2.5, and EDGARv8.0). In specific years, EDGAR emissions (only related to anthropogenic emissions) exceeded those reported by GFEDv4.1s and GFASv1.2 for CO_2 and CH_4.

According to data provided by the three inventories reporting wildfire emissions (i.e. GFEDv4.1s, GFASv1.2, FINN 2.5) a large inter-annual variability affected OVF emissions, with a possible link with the occurrence of La Niña events, stressing the impact of climatic variability on wildfire activity. The primary contributors to emissions varied over time, with countries such as Italy, Algeria, and Greece frequently dominating the considered Mediterranean region. In 2012, GFED and FINN attributed 27% and 35% of CH_4 emissions to Italy, respectively. Conversely**,** CAMS identified Algeria as the highest emitter, contributing by 32% in the considered domain. Our results highlight the need to improve emission inventories by integrating satellite measurements with ground-based data to increase the accuracy and consistency of climate-altering emissions related to OVFs.

Keywords: Open Vegetation Fires, Greenhouse Gases, Black Carbon, Emission Inventories, Mediterranean Region, Climate Change, Wildfire Emissions

1. Introduction

Since the 19th century, anthropogenic activities have led to a continuous upward trend of greenhouse gas (GHG) emissions [1], affecting various aspects of climate, including surface air and ocean temperatures, precipitation, and sea levels. In 2022, global GHG emissions reached a new high of 53.8 Gt of CO_2 equivalent, according to the latest Emissions Database for Global Atmospheric Research (EDGARv8.0) statistics [2]. In 2015, the Paris Agreement established emission targets to keep the rise in global temperature within 1.5°C above pre-industrial levels [3].

According to the latest World Meteorological Organization GHG bulletin [4], the three main GHGs, carbon dioxide (CO_2), methane (CH_4), and nitrous oxide (N_2O) in 2022 have increased, relative to 1750, by 150, 264, and 124%, respectively. Biomass burning (BB) related to open vegetation fires (OVFs) is a relevant source for all of them [5, pp. 2001–2017] [6]. As stated in the study [7], it should be noted that changes in the ecosystem dynamics due to climate change may add further uncertainty to the impact of wildfires on the decadal carbon cycle.

OVFs also emit dangerous pollutants such as particulate matter (PM), carbon monoxide (CO), nitrogen oxides (NO_x), sulfur dioxide (SO_2), and volatile organic compounds (VOCs), which can harm human health and ecosystems [8] [9] [10]. PM is also

associated with major climatic impacts via aerosol-radiation and aerosol-cloud interactions [11]. Globally, BB contributes nearly 30-40% of black carbon (BC) and 90% of primary organic aerosol (POA) emissions, resulting in approximately 34 Tg yr^{-1} of the aerosols in the atmosphere annually [12]. With global emissions between 4800-7200 Gg yr^{-1}, BC, which is the radiation-absorbing component of PM, impacts the climate by heating the atmosphere, accelerating ice melt, and altering cloud properties [13] [14] [15].

According to Hamilton et al. [16], reassessment of pre-industrial fire emissions has been shown to have a significant impact on anthropogenic aerosol forcing. In Europe, OVFs have been linked to climate variability and change (e.g.[17], [18]), with anthropogenic influences being a major component. Increasing aridity has been observed to push Mediterranean forest post-fire recovery towards open shrublands [19], aggravating the frequency and intensity of fires in this region as predicted by non-stationary climate-fire models due to global warming [20]. Wildfires and prescribed burns (controlled fires used for forest management, see [21]), the two main types of OVFs that occur most frequently in Europe, both contribute to pollutant and GHG emissions. Wildfire intensity is driven by climate change, fuel accumulation, expanding human settlements, flammable vegetation, and prolonged burning [8].

The Euro-Mediterranean southern region, where the climate is warmer and drier and considered a future climate ‘hot spot’, is where wildfires in Europe occur (and will occur) most frequently [22] [23] [24].

OVF emissions are not as well characterized as other anthropogenic emissions due to the high variability in time and space, the different factors driving activity and emission efficiency [25], including the size and the stage of the fires, the type of vegetation being burned, weather conditions, and human intervention [26].

Researchers have developed several methodologies to estimate OVF emissions that can be broadly classified according to the approach they use as "bottom-up" or "top-down" [27]. The “bottom-up” approach is based on the combination of geophysical (e.g. type of vegetation within a region, proportion of vegetation burned) and biophysical (emission factors) information. The so-called “top-down” approach uses direct atmospheric observations to quantify the net emissions associated with specific source regions.

To effectively estimate the impact of OVFs on climate, it is essential to have a thorough understanding of the relative performance of different approaches, although each has strengths and limitations. Despite the critical role of fires as a source of GHGs and BC, to our knowledge there is little specific information on OVF emissions in the Mediterranean region. For this reason, this paper aims to review existing methodologies to quantify GHG and BC emissions from OVFs and analyze data provided by four state-of-the-art emission inventories related to OVF emissions of CO_2, CH_4, N_2O, and BC for the Mediterranean region in the period 2003-2020. The paper is structured as follows: in section 2, we discuss the methods used to calculate the emissions, which include satellite observations, ground-based measurements, and modelling techniques. In section 3, we focus on OVFs and GHG emissions in the Mediterranean region by

examining and comparing estimates from different inventories. Section 4 contains discussions on emission estimates and section 5 reports our conclusion.

2. Methods used for estimating greenhouse gas emissions from OVFs: an overview

In this section, we broadly describe two widely used approaches to quantify GHG and BC emissions from OVFs: the so-called “bottom-up” and “top-down” approaches.

2.1 Bottom-Up

OVFs can be classified as wildfires, agricultural waste burning (AWB), or biomass burning (BB). In the bottom-up approach, emissions are derived based on activity data (e.g. area burned, fuel consumption) and emission factors (EF) (i.e. a coefficient that describes the rate at which a given activity releases a certain molecule into the atmosphere). This approach is commonly used by environmental scientists and policymakers, offering transparency and replicability in calculating emissions’ contribution for specified areas.

A bottom-up system for quantifying OVF emissions consists of several interrelated modules, each of which provides specific information for a comprehensive emission estimate [28, pp. 1997–2016]. These modules include the detection of burned areas using satellite data such as the Visible Infrared Imaging Radiometer Suite (VIIRS) (a sensor onboard the polar-orbiting Suomi National Polar Orbiting Partnership; Suomi NPP, NOAA-21 and NOAA-21 weather satellites) or the Moderate Resolution Imaging Spectroradiometer (MODIS) (a key instrument on board the Terra and Aqua satellites),

the calculation of fuel consumption based on biomass burned per unit area and the implementation of emission factors to convert biomass into specific trace gas and aerosol emissions. Temporal distribution modules consistently distribute monthly emissions into daily and hourly values, taking into consideration fire spread rates and diurnal trends. Module outputs are then aggregated into a geospatial framework that maps emissions across landscapes. These components interact through data integration and module calibration to ensure consistency with empirical data and remote sensing. The system provides a comprehensive understanding of the wildfire impacts, including spatially explicit and temporally resolved emissions estimates. By incorporating burned area, fuel consumption, combustion completeness, emission variables, and temporal distribution, the bottom-up system improves our ability to monitor and manage the environmental and air quality impacts of wildfires, as shown in Figure 1.

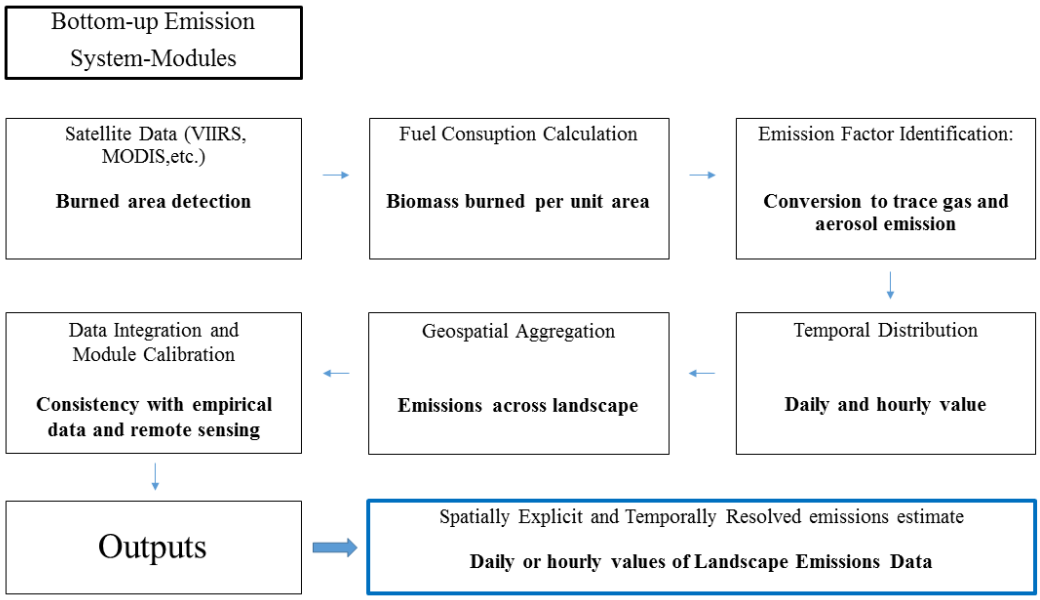

Figure 1: Diagram Illustrating the Modular Structure of a Bottom-Up Emission System for Quantifying Open Vegetation Fire Emissions.

Several studies have used a bottom-up approach to estimate GHG, including CO_2, CH_4, and N_2O emissions from OVFs in Europe.

A study by Rosa et al. (2011) [29], estimated atmospheric emissions from wildfires in Portugal from 1990 to 2000. The researchers used Landsat-based burnt area maps, land cover maps, national forest inventory data, biometric models, and emissions factors from literature. Emissions were calculated based on the area burnt, biomass loading, combustion factor, and emission factor specific to land cover types. The results showed a strong correlation between the area burnt and the emissions, with the combustion factor for shrubs and emission factors identified as the primary sources of uncertainty compared to other sectors, wildfire emissions constitute 1% to 9% of Portugal's total annual GHG emissions.

Volkova et al. [30] enhanced Australia's GHG emissions reporting from forest fires using a Tier 2 approach from the 2006 IPCC Guidelines. They refined the emission estimate equations and incorporated detailed, country-specific data from literature reviews and field measurements. This included improvements in parameters such as the area burned, fuel mass, combustion factors, and emission factors. Additionally, they transitioned to a more accurate model for dead organic matter recovery. These refinements aimed to provide precise GHG emission estimates.

2.2 Top-Down

The "top-down" approach is a method in which atmospheric observations are used to improve the emission estimates of the atmospheric species of interest. This approach estimates emissions utilizing a framework that integrates atmospheric observations, an atmospheric chemical transport model (CTM), and an inversion algorithm. This approach is based on the relationship between atmospheric concentration or mole fraction with emissions, i.e. the so-called ‘source-receptor relationships’ calculated by the CTM. The top-down method uses a “bottom-up” inventory as prior knowledge and optimizes it to match the modelled concentrations with observations. By leveraging the combined information from both “bottom-up” estimates and observations, the inverse modelling approach significantly reduces uncertainties in the posterior emission estimates [31]. The accuracy of these inverse modelling results and the spatial scale at which emission estimates are made depending on the quality and spatial density of measurements and the precision of the transport model used in the analysis [32].

Modelled mixing ratios corresponding to the observations can be calculated as:

$$y^{mod} = Hx \qquad (1)$$

where y^{mod} is a vector of modelled mixing ratio, x is the unknown emission flux vector and H is the source receptor relationship matrix. The emissions fluxes vector x includes the variables to be optimized by the inversion, that is, gridded emissions and other elements such as background mixing ratio values.

Observed values can be expressed as:

$$y^{obs} = Hx + \varepsilon \qquad (2)$$

where y^{obs} is the observation vector and ε represents the observation error. However, observations might not be sufficient to precisely constrain all components of the

emission vector. This situation leads to an ill-conditioned problem, requiring regularization or the introduction of supplementary information to obtain a meaningful solution. Typically, this additional constraint is provided as a priori estimates of the unknowns, that is spatially distributed information of the fluxes (x_b) , obtained from the bottom-up emission estimate.

Following Bayes' theorem, the most likely solution of the posterior emission flux (x) minimizes the difference between the observed and modelled mixing ratios. Assuming that the observation and prior uncertainties follow Gaussian probability density functions, this can be formulated as a cost function:

$$J(x) = \frac{1}{2}(x - x_b)^T B^{-1}(x - x_b) + \frac{1}{2}(Hx - y^{obs})^T R^{-1}(Hx - y^{obs}) \quad (3)$$

In this equation, *B* represents the prior flux error covariance matrix, and *R* is the observation error covariance matrix.

Several methods can be employed to find the optimum posterior state, defined as the value of *x* for which eq. 3 has a minimum. Common approaches include the analytical inversion [33], Kalman filter [34], 3D-Var (Three-Dimensional Variational Assimilation), and 4D-Var (Four-Dimensional Variational Assimilation) [35] optimization techniques.

Inversion models have evolved very rapidly in recent years, reducing uncertainties in emission estimates. For a long time, the inversion methods were used to optimize the net emissions of the species of interest. However, there have been advancements in the field to accommodate the extraction of the sectorial contributions to the posterior total emissions. In a commonly used and straightforward approach, net fluxes are partitioned to underlying sector-based emissions by scaling fluxes based on the relative

weight of sectors in a prior inventory [36]. This does not assume that the prior distribution of sectoral emissions is correct, only that the relative allocation within a given grid cell is correct. A similar approach accounts for emissions from different sectors having different prior error standard deviations contributing differently to each sector [37]. In another approach [38], the state vector is split into different emission sources, such as wetland and non-wetland emissions. It allows the emission sector with higher uncertainty to be treated differently than the well-known sector. In a similar approach [39], the state vector is organized in three ways to obtain monthly, sectorial, and provincial emissions according to the subnational boundaries for each year. Assuming relative weights of different sectors in prior emissions imposes a correlation between emission sectors that may not exist. A study by Cusworth et al. [40] shows a method that projects inverse CH_4 fluxes directly to emission sectors while accounting for uncertainty structure and spatial resolution of prior fluxes and emissions. This method can also be useful in partitioning highly uncertain biospheric and anthropogenic emissions to reconcile the global budget.

In more sophisticated approaches to get accurate sectorial estimates, the inversion system is generally provided with some additional constraints. For instance, to constrain CH_4 fluxes, additional trace gases can be employed to partition emissions. This method becomes feasible when these trace gases are co-emitted from a specific source at a characteristic ratio. For example, carbon monoxide (CO) is emitted alongside CH_4 during incomplete combustion processes [41]. Consequently, CO measurements can be utilized to estimate emissions from activities such as biomass burning. Similarly, ethane (C_2H_6) is emitted during fossil fuel production and use, without significant emissions

from biogenic sources (e.g. [42], [43]). Thus, measurements of C_2H_6 can be valuable in quantifying emissions specifically originating from fossil fuel sources. Observations of isotopologues can also be harnessed to apportion emissions through a similar approach. This method involves evaluating the ratios of isotopologues emitted from different source types. In X.Lan et al. [44], methane isotopologue measurements are used to better understand and differentiate emissions from various sources, including biomass burning emissions. Analyzing these isotopic signatures provides valuable information on the sources and a more comprehensive understanding of methane emissions.

3. Quantification of OVF emissions over the Mediterranean basin: a multi-inventory assessment

To investigate GHG emissions of OVFs in the Mediterranean region, we considered four global and regional emission inventories, which provide essential data for understanding the dynamics of fire-related emissions. In this section, we first describe the considered inventories and then quantify OVF emissions of CO_2, CH_4, N_2O, and BC for the Mediterranean region. Table 1 summarizes key characteristics of the considered inventories, including their acronyms, versions, producers, coverage details, resolutions, formats, data access portals, and foundational reference papers. More specific details about each inventory are provided in the supplementary material.

Table 1: Comparative overview of global fire emission inventories considered in this analysis.

Features	CAMS GFAS	GFED 4.1s	EDGAR v8.0	FINN
Name	CAMS Global Fire Assimilation System	Global Fire Emissions Database Version 4.1	Emissions Database for Global Atmospheric Research Version 8.0	Fire INventory from NCAR
Acronym	GFAS	GFED 4.1s	EDGARv8.0	FINN
Version	V1.2	4.1	8	2.5
Producer	Copernicus Atmosphere Monitoring Service	ORNL DAAC (Oak Ridge National Laboratory Distributed Active Archive Center)	Joint Research Centre (JRC) in collaboration with the International Energy Agency	National Center of Atmospheric Research (NCAR)
Spatial Coverage	Global	Global	Global	Global
Temporal Coverage	From 1 January 2003-present	June 1995 - present	Up to 2022	2002-present
Spatial Resolution	0.1°x0.1°	0.25°x0.25°	0.1°x0.1° and country level	1 km x 1 km
Temporal Resolution	Daily Averages	Monthly, with some daily and 3-hourly data	Annually	Daily
Format	GRIB, with optional conversion to netCDF	HDF5, with some datasets in HDF and text formats	NetCDF and xlsx	HDF5, NetCDF, etc
Source/Data Portal	https://atmosphere.copernicus.eu/global-fire-emissions	http://www.globalfiredata.org/	https://edgar.jrc.ec.europa.eu/	https://rda.ucar.edu/datasets/ds312.9/
Reference Papers	Samuel Rémy, Andreas Veira, Ronan Paugam, et al., 2017	Dave van Wees, Guido R. van der Werf, James T. Randerson, et al., 2022	Tomas Artes, Duartee Oom, Daniele de Rigo, et al., 2019	Christine Wiedinmyer, Yosuke Kimura, Elena C. McDonald-Buller, et al., 2023
	Francesca Di Giuseppe, Samuel Rémy,	S. K. Akagi, R. J. Yokelson, C. Wiedinmyer, et al., 2011	Giacomo Grassi, Giulia Conchedda, Sandro Federici, et al., 2022	C. Wiedinmyer, S. K. Akagi, R. J. Yokelson, et al., 2011

	Florian Pappenberger, et al., 2017			

3.1 Quantification of OVF emissions over the Mediterranean region

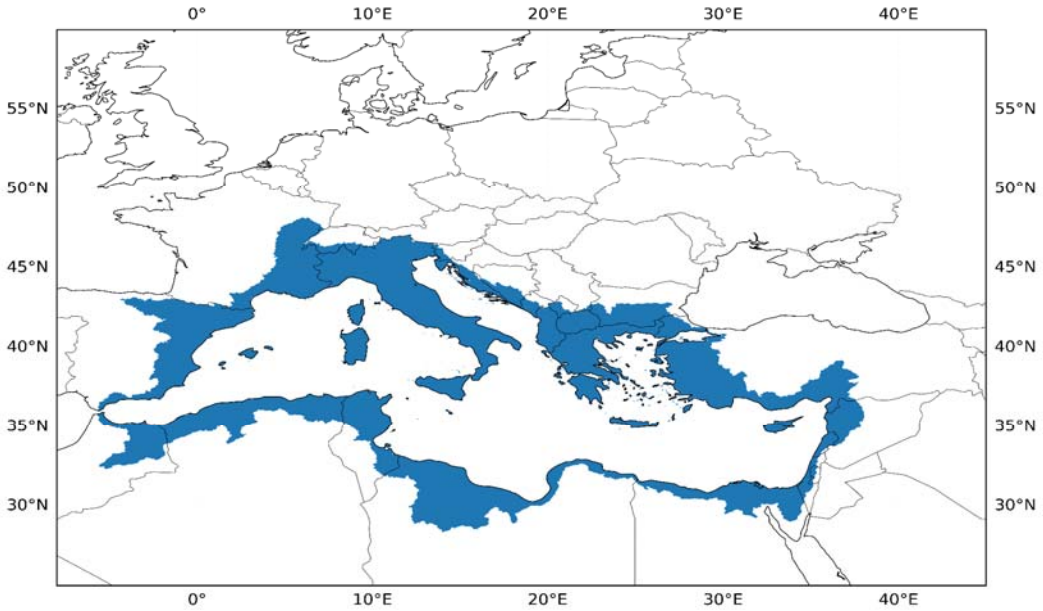

Figure 2: The Mediterranean region domain used to aggregate emission fluxes from CAMS, GFED, FINN and EDGAR emission inventories.

We compare the OVF emissions from the CAMS, GFED, FINN, and EDGAR inventories for the Mediterranean region from 2003 to 2020. Figure 2 shows the Mediterranean region we have considered for the aggregation of emissions, based on WWF HydroSHEDS [45]. A portion of the Nile watershed was also included. A raster mask

was obtained by clipping the Koeppen climate classification map at 0.083° res from Beck et al., 2018 [46]. An alternative study area was obtained by removing the montane climate area from the resulting map (classes 15, 26, 27, 29, 30) within the watersheds. The blue highlighted area of the countries included in this defined domain is referred to as the Mediterranean Region in our analysis.

The Mediterranean domain we considered constitutes approximately 1.5% of the land area with respect to the global land area. Using the global CO_2 emissions provided by [47] as a reference, during the study period, the percent contribution of the Mediterranean Region to global OVF emissions ranged from a minimum of 0.18-0.32% in 2012 to a maximum of 0.24-0.45% in 2007. It must be noted that these figures refer to our domain, as defined above, and can change as a function of the spatial domain selected to represent the Mediterranean region. As an instance, including the whole Iberian peninsula in the analysis (as done e.g. by Gudmundsson et al. 2014; and by Turco et al. 2017) would increase the relative values.

Figure 3 reports the multi-annual variability of open fire emissions for CO_2, CH_4, N_2O, and BC over the Mediterranean region from 2003 to 2020. Note that GFED, CAMS, and FINN include anthropogenic and natural vegetation fires, whereas EDGAR only includes anthropogenic emissions related to agricultural practices.

The GFED, CAMS, and FINN inventories show consistency in identifying temporal peaks in the emissions, although there are differences in the absolute values, with CAMS and FINN often showing emission levels higher than GFED. EDGAR showed higher CO_2 emission values than GFED for 10 out of 18 years. This is surprising, as

EDGAR is expected to represent a lower limit for emissions, as it only reports agriculture vegetation fires.

In 2007, extreme fire danger conditions affected south-eastern Europe at the end of July and August [48]. These conditions led to catastrophic events affecting southern Italy and Greece, with record numbers of burnt areas. In 2007, the Rapid Damage Assessment module of the European Forest Fires Information System (EFFIS) reported high burnt areas for Greece (271,516 ha) and Italy (153,753 ha) [49]. The weather conditions that contributed to the wildfires included prolonged heat waves with very high temperatures, a prolonged drought that preceded the events, and strong winds that coincided with the ignition of the fire [50]. In 2017, as reported by the European Drought Observatory, Italy experienced a severe drought in 2017, followed by one of the driest springs in the country in the last 60 years. During this period, some regions received 80% less rainfall than normal. Two-thirds of Italy was affected by these conditions [51] leading to a high burnt area (140,404 ha, with 788 fires) [52].

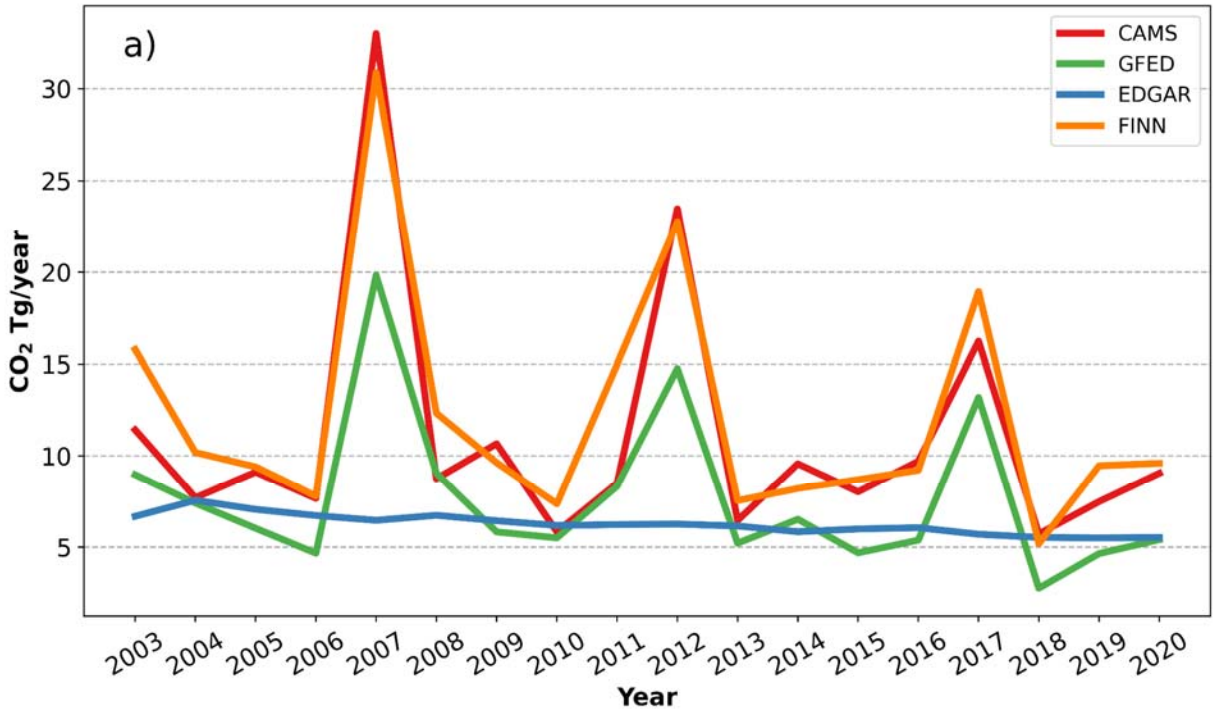
a)
CAMS
GFED
EDGAR
FINN
CO_2 Tg/year
30
25
20
15
10
5
2003
2004
2005
2006
2007
2008
2009
2010
2011
2012
2013
2014
2015
2016
2017
2018
2019
2020
Year

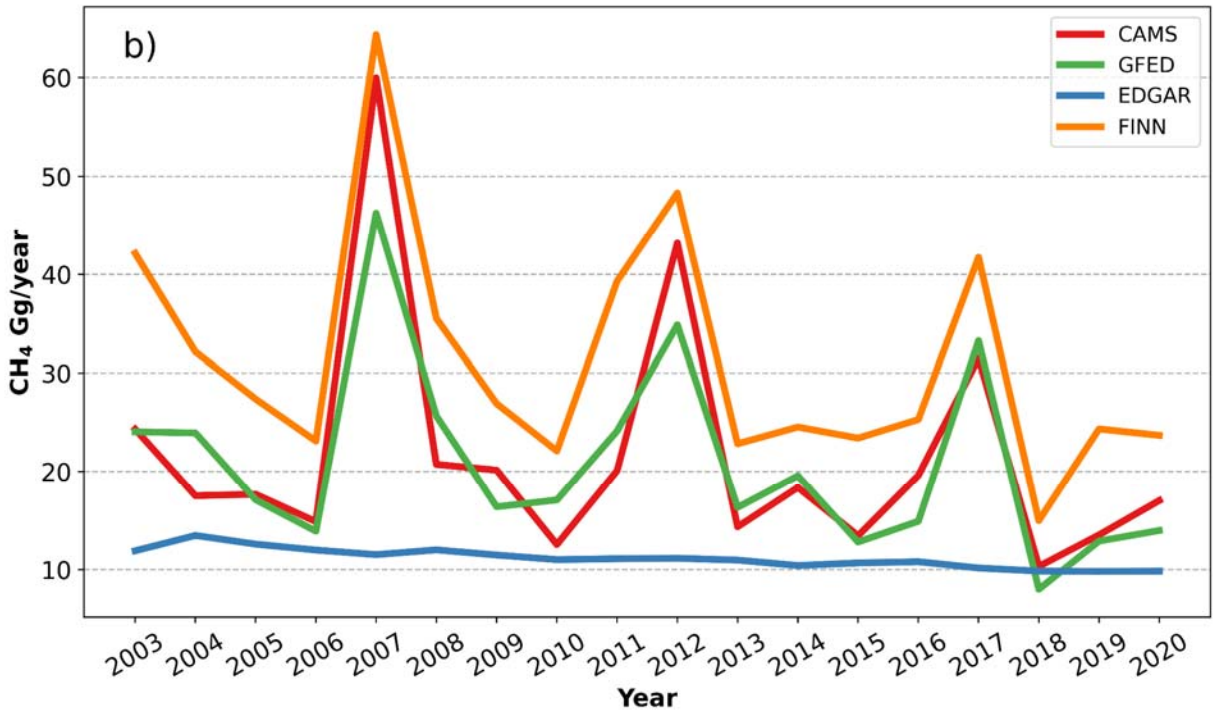
b)
CAMS
GFED
EDGAR
FINN
CH_4 Gg/year
60
50
40
30
20
10
2003
2004
2005
2006
2007
2008
2009
2010
2011
2012
2013
2014
2015
2016
2017
2018
2019
2020
Year

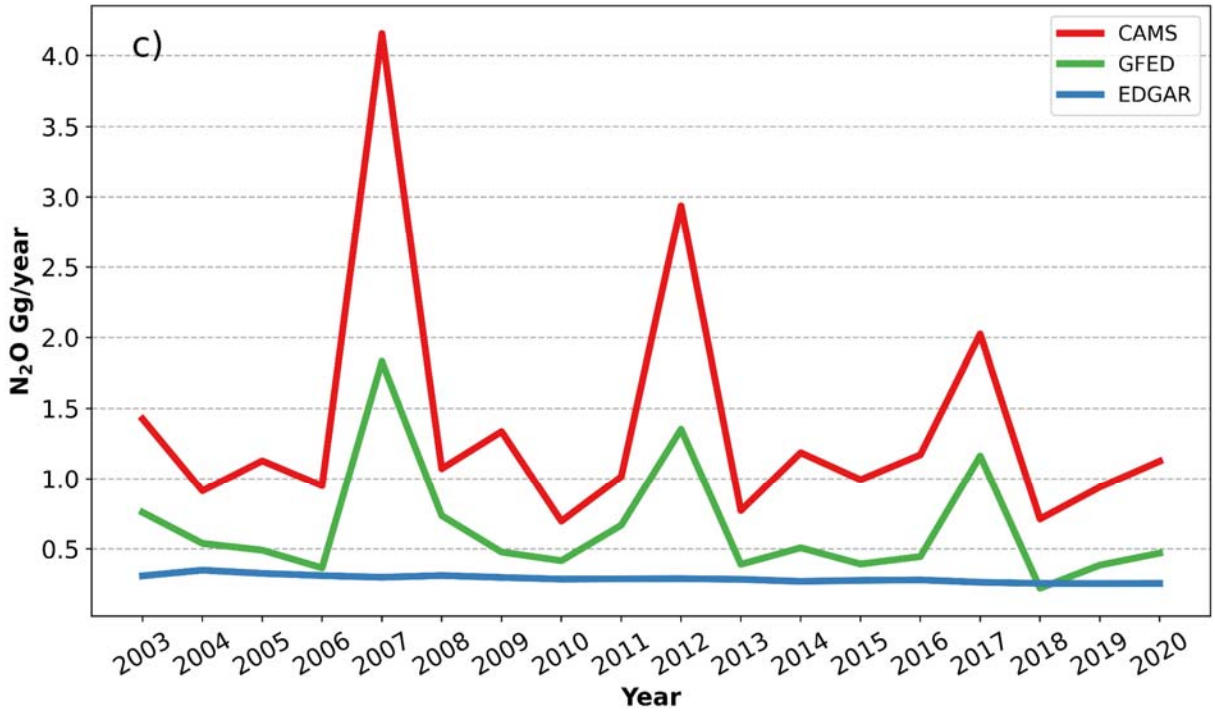
c)
CAMS
GFED
EDGAR
4.0
3.5
3.0
2.5
2.0
1.5
1.0
0.5
N2O Gg/year
2003
2004
2005
2006
2007
2008
2009
2010
2011
2012
2013
2014
2015
2016
2017
2018
2019
2020
Year

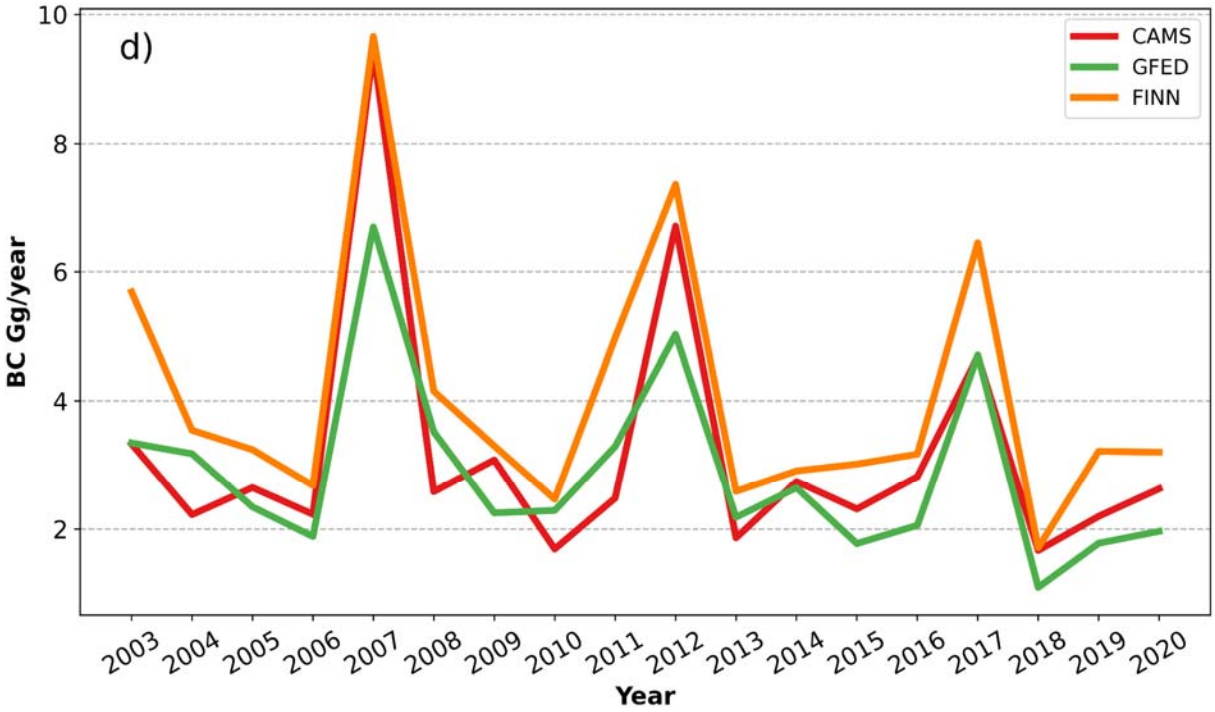
d)
CAMS
GFED
FINN
10
8
6
4
2
BC Gg/year
2003
2004
2005
2006
2007
2008
2009
2010
2011
2012
2013
2014
2015
2016
2017
2018
2019
2020
Year

Figure 3: Annual emissions from OVFs in the Mediterranean region (2003-2020): CO_2 (a), CH_4 (b), N_2O (c) and BC (d). The different lines denote CAMS (red), GFED (green), EDGAR (blue), and FINN (orange).

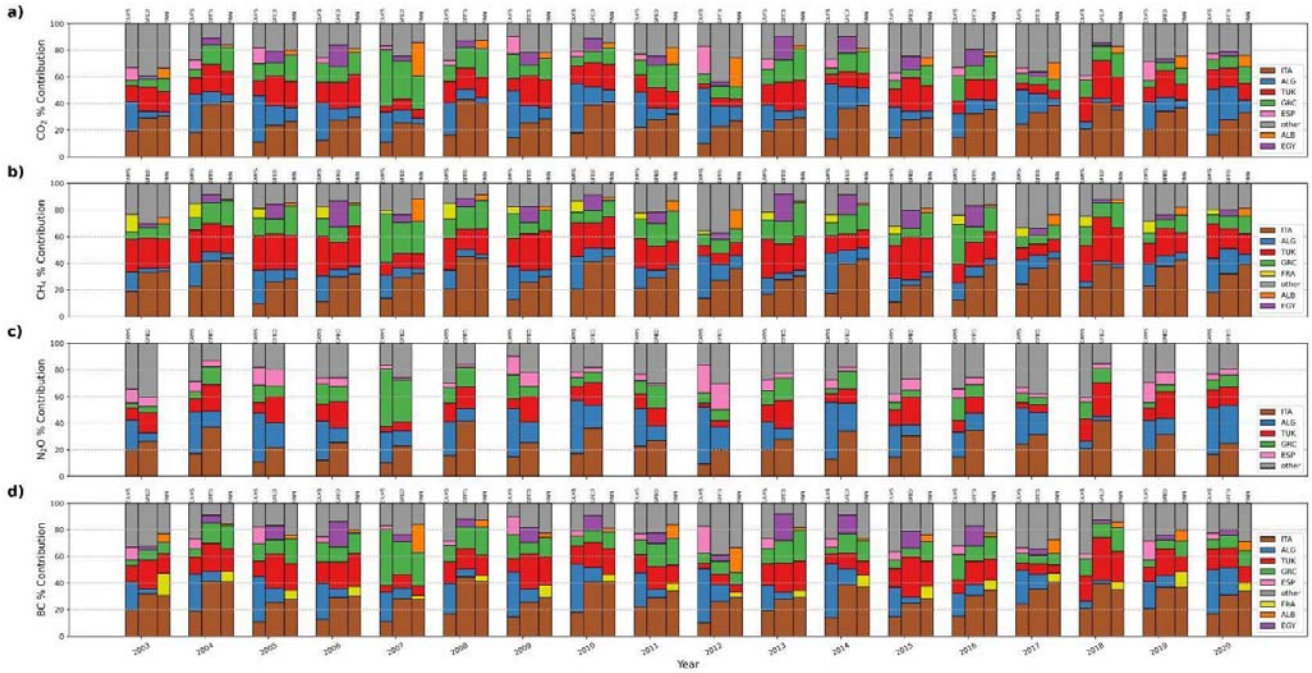

Figure 4: Annual emissions for CO_2 (a), CH_4 (b), N_2O (c), and BC (d) split for the 8 top emitters are reported (Albania: ALB, Algeria: ALG; Egypt: EGY; France: FRA; Greece: GRE; Italy: ITA; Spain: ESP, Turkey: TUR; other countries: OTH). Please note that only data from GFEDv4.1s, GFASv1.2, and FINN 2.5 were considered.

Figure 4 shows the percentage of contributions of different countries to the GHG and BC emissions from the Mediterranean region over the period 2003-2020. It is important to emphasize that we refer only to the area of each country that is included within the borders of the domain reported in Figure 2. Italy, Algeria, and Greece are the main

contributors to emissions in all the years considered. This is not surprising considering that these countries have the largest spatial area in the analyzed domain.

Looking at the years characterized by the emission peaks (i.e. 2007, 2012, and 2017), we observed not negligible differences in the emission shares derived by GFED, CAMS, and FINN.

For CO_2 emissions, in 2007 and 2012, CAMS showed Algeria as the top contributor (22% and 41% of total emissions), GFED reported Italy as the top contributor (25% and 22% of the total emissions) and FINN also reported Italy as the top contributor (25% and 27% of total emissions). For 2017, all considered inventories show Italy as the main contributor with 24% of the total emissions reported by CAMS, 33% of the total emissions reported by GFED, and 39% of the total emissions reported by FINN. A notable difference is that CAMS reported Spain as one of the main Mediterranean contributors for each year, while GFED reported Egypt and FINN reported Albania.

For CH_4 in 2007, CAMS showed Greece as the top contributor (38% of total emissions). GFED reported 29% of the total emission contribution from Italy and 23% from Greece. However, FINN reported 32% of the total emission contribution from Italy and 24% from Greece. For 2012, CAMS reported Algeria (32% of total emissions) as the top contributor for CH_4, while GFED suggested that Italy (27% of total emissions) dominated the total emissions and FINN also reported Italy as the top contributor (35% of total emissions). For 2017, the results are consistent for all three inventories showing Italy as the main contributor. Again a notable difference can be seen when CAMS reported France as one of the top Mediterranean contributors, while GFED reported Egypt and

FINN reported Albania. The most important thing to note is that for 2007, 2012, and 2017, major fires in Egypt were not reported by EFFIS [49] [52] [53], which is not consistent with figures reported by GFED.

For N_2O in 2007, both CAMS and GFED reported Greece (43% and 34% of total emissions, respectively) as the largest contributor; the second largest contributor was Algeria (23% of total emissions) for CAMS and Italy (23% of total emissions) for GFED. For 2012, CAMS reported Algeria (45% of total emissions) as the top contributor, while GFED reported Italy (22% of total emissions). FINN did not report N_2O emissions.

In examining trends of BC emissions, contrasting outputs were observed between the CAMS, GFED, and FINN inventories. Specifically, CAMS identified Spain as a significant source of emissions, GFED highlighted Egypt and FINN highlighted Albania. Instead of Algeria, reported by CAMS and GFED, FINN also highlighted France as one of the major emission contributors for BC. Although all three inventories tracked the inter-annual variability of BC emissions, their findings are not consistent, as shown by the differences in the reported emission percentages and the listed top contributors of the emissions by each inventory. This discrepancy underscores the challenges of reconciling data across different inventories and highlights the need for further scrutiny of the methodologies adopted by each inventory.

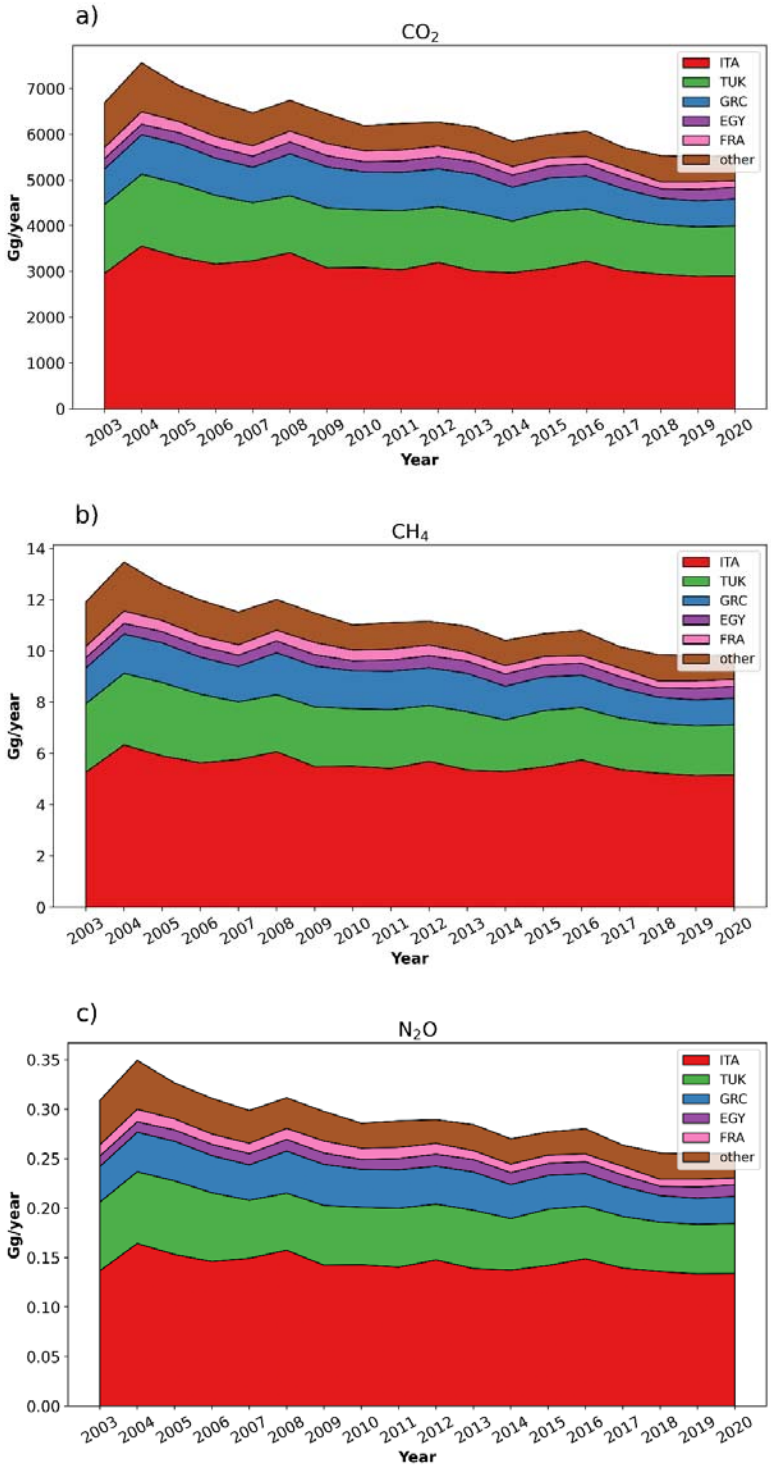

Figure 5: Agriculture and Waste Burning (AWB) Emission trends reported by EDGARv.8

EDGARv8 AWB CO_2, CH_4, and N_2O emissions were analyzed from 2003 to 2020. (Figure 5). Clear patterns emerge when the data are grouped into three consecutive 5-year periods. Table 2 reports the CO_2, CH_4, and N_2O emission trends by the top 5 emitting countries in the respective domain.

Over the period 2005-2020, France (36%), Greece (32%) and Turkey (31%) showed significant reductions in GHG emissions. Italy showed a moderate reduction (12%), while Egypt showed a slight increase in emissions. This reduction of the emissions from the European countries in the domain can be attributed to the implementation of directives defined to control AWB, as highlighted by the United Nations Economic Commission for Europe and supported by the European Union's sustainable waste management policies.

Table 2: Trends in CO_2, CH_4, and N_2O emissions by top 5 emitting countries within the domain, 2005-2020: A comparative overview of mean annual emissions for EDGARv8 emission.

CO_2 Emissions			
Country	**2005-2010 Mean (Tg/year)**	**2011-2015 Mean (Tg/year)**	**2016-2020 Mean (Tg/year)**
ITA	3.22	3.06	3.0
TUK	1.37	1.23	1.11
GRC	0.85	0.80	0.62
FRA	0.24	0.21	0.17
EGY	0.24	0.26	0.24
Other	0.69	0.55	0.54
CH_4 Emissions			

Country	2005-2010 Mean (Gg/year)	2011-2015 Mean (Gg/year)	2016-2020 Mean (Gg/year)
ITA	5.73	5.45	5.34
TUK	2.43	2.19	1.97
GRC	1.51	1.42	1.11
FRA	0.43	0.37	0.3
EGY	0.43	0.46	0.43
Other	1.23	0.97	0.95
N_2O Emissions			
Country	**2005-2010 Mean (Gg/year)**	**2011-2015 Mean (Gg/year)**	**2016-2020 Mean (Gg/year)**
ITA	0.15	0.14	0.14
TUK	0.06	0.06	0.05
GRC	0.04	0.04	0.03
FRA	0.01	0.01	0.01
EGY	0.01	0.01	0.01
Other	0.03	0.03	0.02

4. Discussion on emission estimates

As reported in Section 3.1 a ~5-year periodicity is evident in the emissions of GHGs and BC diagnosed by the inventories which considered wildfire contributions (i.e. GFEDv4.1s, GFASv1.2, and FINN 2.5). Forest fires are a complex process associated with factors of different origins and occurring on different spatial and temporal scales, such as vegetation and landscape conditions, climate and weather, and human activities [54]. It is thus difficult to quantify and univocally attribute the relative importance of these different processes to fire occurrences and related emissions.

However, previous studies (e.g. Meyn et al. [55]) suggested that climatic processes, through their impact on fuel moisture, as well as on nature and availability of fuel, can represent a driving process for the inter-annual variability of regional fire patterns, especially in the Mediterranean region. In particular, a ~5-year periodicity in the burned areas was observed by Turco et al. [20] for the northeastern Iberian Peninsula related to summer precipitation and maximum temperature as well as antecedent climate conditions with a time lag of 1-2 years. From this perspective, it is interesting to note that all the years that are characterized by a peak in OVF emissions over the Mediterranean basin are featured by the occurrence of La Niña events. La Niña represents the “cold ” phase of the El Niño Southern Oscillation (ENSO), a quasi-periodic (two to seven years) climate pattern affecting the equatorial Pacific circulation [56]. It is the primary cause of fluctuations in the terrestrial carbon cycle, particularly in the tropics [57]: previous studies [58] [59] suggested a significant global influence of ENSO on the carbon budget by increased fire activity and decreased terrestrial carbon sink capacity.

For the Asia-Pacific region, ENSO has been an important climate driver, but its influence over North Atlantic Europe is quite challenging to establish [60] [61], despite previous research suggesting a robust climate influence over Europe [62].

The South Asian summer monsoon and ENSO are closely related through atmospheric teleconnections. ENSO modulates the strength and intensity of monsoons with la Niña events leading to stronger monsoons. This variability in the monsoon, in return, impacts the Mediterranean climate through the monsoon-desert mechanism, affecting subsidence and precipitation patterns in the region. In the years with a stronger

monsoon, there is a noticeable increase in the vertical advection of moist static energy and horizontal advection of dry enthalpy over the Mediterranean region, leading to drier conditions [63].

According to NOAA [64], years can be classified as “weak”, “moderate”, “strong”, or “very strong” for what concerns the magnitude of ENSO. According to the NOAA classification, the 2007-2008 event was categorized as “strong” ENSO, the 2011-2012 event as “moderate”, and the 2017-2018 event as “weak”. Thus, we argue that ENSO may have played a role in determining the observed inter-annual variability of GHG and BC emissions associated with OVF in the Mediterranean region. Nevertheless, it should be noted that our integrated basin perspective prevented us from considering specific emission variability that can occur among different source regions (see e.g. [65]). Moreover, the availability of annually integrated emission values did not allow us to investigate the seasonal variability of emissions.

Despite their agreement on the diagnosis of emission peak years, there were notable differences in the quantification of total GHG and BC emissions in the Mediterranean for GFED, CAMS, and FINN. The differences between the inventories, especially in the identification of the main contributors of GHG emissions (Italy, Algeria, and Greece, with uncertainties including France and Egypt), suggested further efforts in reducing underlying uncertainties. These discrepancies not only highlight the issue of the accuracy of emission estimates but also hamper efforts to implement effective climate change mitigation policies in the Mediterranean region.

Table 3: Average standard deviation (σ) and average normalized standard deviation (coefficient of variation, v) for ITA, ALG, GRC, and the whole study domain for different atmospheric species. σ is in Tg for CO_2 and in Gg for all other species.

Species	ITA		ALG		GRC		Med	
	σ	v	σ	v	σ	v	σ	v
CO_2	1.04	0.37	1.4	0.91	1.21	0.45	3.63	0.27
CH_4	3.34	0.45	1.9	0.76	2.3	0.54	8.72	0.34
N_2O	0.06	0.23	0.21	1.04	0.18	0.55	0.57	0.56
BC	0.4	0.39	0.36	0.6	0.27	0.41	0.68	0.19

For most species considered, the emission inventories showed good agreement. To assess the spread of the four emission inventories, we calculated the average standard deviation (σ) and the average normalized standard deviation (coefficient of variation, v) for the study period for the top three emitting countries and the entire study domain (Table 3). The σ parameter provides indication about the temporal variability of emissions during the investigation period. The coefficient of variation (v) can be used as a measure of the emission spread across the different inventories for the species. Emissions for Algeria are highly variable across all species. BC emissions are the most consistent, while N_2O emissions show the highest variability across inventories. Overall, the variability for all gases highlights the need for standardized methods and

harmonization among inventories to improve the reliability and consistency of emissions data. Our analysis is consistent with recent scientific discussions highlighting the need to align emission inventories to achieve greater accuracy [66] [67]. It is noteworthy that, based on the literature review presented in this work, no emission estimates from atmospheric inversion modelling exist so far for OVF emissions in the Mediterranean region. Working on the application of this methodology would represent a valuable contribution towards a better quantification (and reduction) of the uncertainties associated with the inventories used to constraint emission estimates in this work.

5. Conclusions

This work reviewed the current methodologies for quantifying climate-altering emissions from OVFs in the Mediterranean region, focusing on CO_2, CH_4, N_2O, and BC. This study revealed significant deviations in emission estimates from four widely used inventories (GFEDv4.1s, GFASv1.2, FINN 2.5**,** and EDGARv8.0), underlying the constraints and limitations on the accounting of climate-altering emissions for this sector. Assuming that the variability among inventories can be considered as a measure of underlying uncertainties in the total emissions, the differences between the inventories, especially in identifying the main contributors of GHG emissions (Italy, Algeria, and Greece, with uncertainties including France and Egypt), suggested further efforts in improving estimates.

OVF emissions in the Mediterranean basin relative to global CO_2 emissions are not constant and exhibit significant variability over the years. Specifically, during the peak years of 2007, 2012, and 2017, there were noticeable increases in absolute emissions.

We hypothesized and discussed the possibility that this variability in the emissions can be related to global climate processes, like ENSO. In order to indicate the role of the Mediterranean region as a global source of OVF emissions, we calculated the contribution to global CO_2 emissions related to OVF for the years with emission peaks.

This study highlights the importance of upgrading GHG emission inventories to better reflect the impact of open fire emissions in the Mediterranean region. It highlights significant differences in the reported emissions and underlines the importance of using standardized, transparent, and verifiable methodologies for GHG accounting.

A further step forward in our analysis would be to analyze the emission variability at sub-regional scales and with (at least) seasonal time resolution. In general, we would recommend that future studies should focus on developing consistent methodologies for quantifying and reporting emissions, integrating satellite measurements with ground-based data through atmospheric inversion modelling as already done for other emission sectors.

Acknowledgments

We would like to thank the teams behind the GFEDv4.1s, GFASv1.2, FINN 2.5, and EDGARv8.0 inventories for providing the crucial data that significantly contributed to our research. We gratefully thank Annalisa Cherchi (CNR - ISAC) for the useful discussion about the role of ENSO in the Mediterranean region. We thank Riccardo Testolin (ISAFOM-CNR and NBFC, Italy) for providing the Mediterranean mask. We acknowledge the support from the University School for Advanced Studies IUSS Pavia

("Scuola Universitaria Superiore IUSS Pavia") and the Institute of Atmospheric Sciences and Climate (ISAC), National Research Council (CNR), Italy.

References

[1] M. Roelfsema *et al.*, "Taking stock of national climate policies to evaluate implementation of the Paris Agreement," *Nat Commun*, vol. 11, no. 1, p. 2096, Apr. 2020, doi: 10.1038/s41467-020-15414-6.

[2] Joint Research Centre (European Commission) *et al.*, *GHG emissions of all world countries: 2023*. LU: Publications Office of the European Union, 2023. Accessed: Oct. 17, 2023. [Online]. Available: https://data.europa.eu/doi/10.2760/953322

[3] "Paris Agreement." Accessed: Jun. 26, 2023. [Online]. Available: https://climate.ec.europa.eu/eu-action/international-action-climate-change/climate-negotiations/paris-agreement_en

[4] "Greenhouse Gas Bulletin." Accessed: Jun. 26, 2023. [Online]. Available: https://public.wmo.int/en/greenhouse-gas-bulletin

[5] Y. Shi *et al.*, "High-resolution and multi-year estimation of emissions from open biomass burning in Northeast China during 2001–2017," *Journal of Cleaner Production*, vol. 310, p. 127496, Aug. 2021, doi: 10.1016/j.jclepro.2021.127496.

[6] P. J. Crutzen and M. O. Andreae, "Biomass Burning in the Tropics: Impact on Atmospheric Chemistry and Biogeochemical Cycles," *Science*, vol. 250, no. 4988, pp. 1669–1678, Dec. 1990, doi: 10.1126/science.250.4988.1669.

[7] J.-S. Landry and H. D. Matthews, "Non-deforestation fire vs. fossil fuel combustion: the source of CO_2 emissions affects the global carbon cycle and climate responses," *Biogeosciences*, vol. 13, no. 7, pp. 2137–2149, Apr. 2016, doi: 10.5194/bg-13-2137-2016.

[8] D. M. J. S. Bowman and F. H. Johnston, "Wildfire Smoke, Fire Management, and Human Health," *EcoHealth*, vol. 2, no. 1, pp. 76–80, Mar. 2005, doi: 10.1007/s10393-004-0149-8.

[9] A. Anav *et al.*, "Meteorological, chemical and biological evaluation of the coupled chemistry-climate WRF-Chem model from regional to urban scale. An impact-oriented application for human health," *Environmental Research*, vol. 257, p. 119401, Sep. 2024, doi: 10.1016/j.envres.2024.119401.

[10] A. De Marco *et al.*, "Strategic roadmap to assess forest vulnerability under air pollution and climate change," *Global Change Biology*, vol. 28, no. 17, pp. 5062–5085, 2022, doi: 10.1111/gcb.16278.

[11] Intergovernmental Panel On Climate Change (Ipcc), *Climate Change 2021 – The Physical Science Basis: Working Group I Contribution to the Sixth Assessment Report of the Intergovernmental Panel on Climate Change*, 1st ed. Cambridge University Press, 2023. doi: 10.1017/9781009157896.

[12] T. C. Bond *et al.*, "Bounding the role of black carbon in the climate system: A scientific assessment," *Journal of Geophysical Research: Atmospheres*, vol. 118, no. 11, pp. 5380–5552, 2013, doi: 10.1002/jgrd.50171.

[13] S. Kang, Y. Zhang, Y. Qian, and H. Wang, “A review of black carbon in snow and ice and its impact on the cryosphere,” *Earth-Science Reviews*, vol. 210, p. 103346, Nov. 2020, doi: 10.1016/j.earscirev.2020.103346.

[14] Z. Klimont *et al.*, “Global anthropogenic emissions of particulate matter including black carbon,” *Atmospheric Chemistry and Physics*, vol. 17, no. 14, pp. 8681–8723, Jul. 2017, doi: 10.5194/acp-17-8681-2017.

[15] “Linking atmospheric pollution to cryospheric change in the Third Pole region: current progress and future prospects | National Science Review | Oxford Academic.” Accessed: Jun. 27, 2024. [Online]. Available: https://academic.oup.com/nsr/article/6/4/796/5370097

[16] “Reassessment of pre-industrial fire emissions strongly affects anthropogenic aerosol forcing | Nature Communications.” Accessed: Jun. 26, 2023. [Online]. Available: https://www.nature.com/articles/s41467-018-05592-9

[17] “(11) (PDF) Spatiotemporal patterns of changes in fire regime and climate: defining the pyroclimates of south-eastern France (Mediterranean Basin).” Accessed: Jun. 26, 2023. [Online]. Available: https://www.researchgate.net/publication/271649184_Spatiotemporal_patterns_of_changes_in_fire_regime_and_climate_defining_the_pyroclimates_of_south-eastern_France_Mediterranean_Basin

[18] P. M. Fernandes, A. M. G. Barros, A. Pinto, and J. A. Santos, “Characteristics and controls of extremely large wildfires in the western Mediterranean Basin,” *Journal of Geophysical Research: Biogeosciences*, vol. 121, no. 8, pp. 2141–2157, 2016, doi: 10.1002/2016JG003389.

[19] M. Baudena *et al.*, “Increased aridity drives post□fire recovery of Mediterranean forests towards open shrublands,” *New Phytologist*, vol. 225, pp. 1500–1515, Feb. 2020, doi: 10.1111/nph.16252.

[20] M. Turco, S. Herrera, E. Tourigny, E. Chuvieco, and A. Provenzale, “A comparison of remotely-sensed and inventory datasets for burned area in Mediterranean Europe,” *International Journal of Applied Earth Observation and Geoinformation*, vol. 82, p. 101887, Oct. 2019, doi: 10.1016/j.jag.2019.05.020.

[21] “Fire and Society: A Comparative Analysis of Wildfire in Greece and the United States on JSTOR.” Accessed: Jun. 30, 2023. [Online]. Available: https://www.jstor.org/stable/24707531

[22] F. Moreira *et al.*, “Landscape – wildfire interactions in southern Europe: Implications for landscape management,” *Journal of Environmental Management*, vol. 92, no. 10, pp. 2389–2402, Oct. 2011, doi: 10.1016/j.jenvman.2011.06.028.

[23] S. Noce, A. Collalti, R. Valentini, and M. Santini, “Hot spot maps of forest presence in the Mediterranean basin,” *iForest - Biogeosciences and Forestry*, vol. 9, no. 5, p. 766, 2016, doi: 10.3832/ifor1802-009.

[24] P. Lionello and L. Scarascia, “The relation between climate change in the Mediterranean region and global warming,” *Reg Environ Change*, vol. 18, no. 5, pp. 1481–1493, Jun. 2018, doi: 10.1007/s10113-018-1290-1.

[25] “Global burned area and biomass burning emissions from small fires - Randerson - 2012 - Journal of Geophysical Research: Biogeosciences - Wiley Online Library.” Accessed: Jun. 26, 2023. [Online]. Available: https://agupubs.onlinelibrary.wiley.com/doi/full/10.1029/2012JG002128

[26] D. N. S. Skowronski, “Multi-scale Analyses of Wildland Fire Combustion Processes in Open- canopied Forests using Coupled and Iteratively Informed Laboratory-, Field-, and Model-based Approaches”.

[27] E. S. Kasischke and J. E. Penner, “Improving global estimates of atmospheric emissions from biomass burning,” *Journal of Geophysical Research: Atmospheres*, vol. 109, no. D14, 2004, doi: 10.1029/2004JD004972.

[28] G. R. van der Werf *et al.*, “Global fire emissions estimates during 1997–2016,” *Earth System Science Data*, vol. 9, no. 2, pp. 697–720, Sep. 2017, doi: 10.5194/essd-9-697-2017.

[29] I. M. D. Rosa, J. M. C. Pereira, and S. Tarantola, “Atmospheric emissions from vegetation fires in Portugal (1990–2008): estimates, uncertainty analysis, and sensitivity analysis,” *Atmospheric Chemistry and Physics*, vol. 11, no. 6, pp. 2625–2640, Mar. 2011, doi: 10.5194/acp-11-2625-2011.

[30] L. Volkova, S. H. Roxburgh, N. C. Surawski, C. P. (Mick) Meyer, and C. J. Weston, “Improving reporting of national greenhouse gas emissions from forest fires for emission reduction benefits: An example from Australia,” *Environmental Science & Policy*, vol. 94, pp. 49–62, Apr. 2019, doi: 10.1016/j.envsci.2018.12.023.

[31] C. D. Rodgers, “Inverse Methods for Atmospheric Sounding: Theory and Practice,” in Series on Atmospheric, Oceanic and Planetary Physics, vol. 2. WORLD SCIENTIFIC, Jul. 2000. doi: 10.1142/3171.

[32] P. Bergamaschi *et al.*, *Atmospheric monitoring and inverse modelling for verification of greenhouse gas inventories*. 2018. doi: 10.2760/759928.

[33] A. Stohl *et al.*, “An analytical inversion method for determining regional and global emissions of greenhouse gases: Sensitivity studies and application to halocarbons,” *Atmospheric Chemistry and Physics*, vol. 9, no. 5, pp. 1597–1620, Mar. 2009, doi: 10.5194/acp-9-1597-2009.

[34] G. Evensen, “The Ensemble Kalman Filter: theoretical formulation and practical implementation,” *Ocean Dynamics*, vol. 53, no. 4, pp. 343–367, Nov. 2003, doi: 10.1007/s10236-003-0036-9.

[35] J. F. Meirink, H. J. Eskes, and A. P. H. Goede, “Sensitivity analysis of methane emissions derived from SCIAMACHY observations through inverse modelling,” *Atmospheric Chemistry and Physics*, vol. 6, no. 5, pp. 1275–1292, Apr. 2006, doi: 10.5194/acp-6-1275-2006.

[36] Z. Qu *et al.*, “Global distribution of methane emissions: a comparative inverse analysis of observations from the TROPOMI and GOSAT satellite instruments,” *Atmospheric Chemistry and Physics*, vol. 21, no. 18, pp. 14159–14175, Sep. 2021, doi: 10.5194/acp-21-14159-2021.

[37] “National quantifications of methane emissions from fuel exploitation using high resolution inversions of satellite observations | Nature Communications.” Accessed: Mar. 27, 2024. [Online]. Available: https://www.nature.com/articles/s41467-023-40671-6

[38] Y. Zhang *et al.*, “Attribution of the accelerating increase in atmospheric methane during 2010–2018 by inverse analysis of GOSAT observations,” *Atmospheric Chemistry and Physics*, vol. 21, no. 5, pp. 3643–3666, Mar. 2021, doi: 10.5194/acp-21-3643-2021.

[39] X. Lu *et al.*, “Methane emissions in the United States, Canada, and Mexico: Evaluation of national methane emission inventories and sectoral trends by inverse analysis of in situ (GLOBALVIEWplus CH₄ ObsPack) and satellite (GOSAT) atmospheric observations,” Aug. 19, 2021. doi: 10.5194/acp-2021-671.

[40] D. Cusworth *et al.*, “A Bayesian framework for deriving sector-based methane emissions from top-down fluxes,” *Communications Earth & Environment*, vol. 2, Nov. 2021, doi: 10.1038/s43247-021-00312-6.

[41] “Comparative inverse analysis of satellite (MOPITT) and aircraft (TRACE-P) observations to estimate Asian sources of carbon monoxide - Heald - 2004 - Journal of Geophysical Research: Atmospheres - Wiley Online Library.” Accessed: Mar. 27, 2024. [Online]. Available: https://agupubs.onlinelibrary.wiley.com/doi/full/10.1029/2004JD005185

[42] J. Peischl *et al.*, “Quantifying sources of methane using light alkanes in the Los Angeles basin, California,” *Journal of Geophysical Research: Atmospheres*, vol. 118, no. 10, pp. 4974–4990, 2013, doi: 10.1002/jgrd.50413.

[43] D. Helmig *et al.*, “Reversal of global atmospheric ethane and propane trends largely due to US oil and natural gas production,” *Nature Geosci*, vol. 9, no. 7, pp. 490–495, Jul. 2016, doi: 10.1038/ngeo2721.

[44] X. Lan *et al.*, “Improved Constraints on Global Methane Emissions and Sinks Using δ13C-CH4,” *Global Biogeochemical Cycles*, vol. 35, no. 6, p. e2021GB007000, 2021, doi: 10.1029/2021GB007000.

[45] “HydroBASINS.” Accessed: Jul. 17, 2024. [Online]. Available: https://www.hydrosheds.org/products/hydrobasins

[46] H. E. Beck, N. E. Zimmermann, T. R. McVicar, N. Vergopolan, A. Berg, and E. F. Wood, “Present and future Köppen-Geiger climate classification maps at 1-km resolution,” *Sci Data*, vol. 5, no. 1, p. 180214, Oct. 2018, doi: 10.1038/sdata.2018.214.

[47] V. Samborska, H. Ritchie, and M. Roser, “Wildfires,” *Our World in Data*, Mar. 2024, Accessed: May 27, 2024. [Online]. Available: https://ourworldindata.org/wildfires

[48] R. Cesari *et al.*, “Modelling dispersion of smoke from wildfires in a Mediterranean area,” *IJEP*, vol. 55, no. 1/2/3/4, p. 219, 2014, doi: 10.1504/IJEP.2014.065927.

[49] Directorate-General for Environment (European Commission), Institute for Environment and Sustainability (Joint Research Centre), A. Camia, J. San-Miguel-Ayanz, and J. Kucera, *Forest fires in Europe 2007*. LU: Publications Office of the European Union, 2008. Accessed: Mar. 07, 2024. [Online]. Available: https://data.europa.eu/doi/10.2788/76413

[50] N. Koutsias, M. Arianoutsou, A. S. Kallimanis, G. Mallinis, J. M. Halley, and P. Dimopoulos, “Where did the fires burn in Peloponnisos, Greece the summer of 2007? Evidence for a synergy of fuel and weather,” *Agricultural and Forest Meteorology*, vol. 156, pp. 41–53, Apr. 2012, doi: 10.1016/j.agrformet.2011.12.006.

[51] “EDO Home - European Drought Observatory - JRC European Commission.” Accessed: Mar. 26, 2024. [Online]. Available: https://edo.jrc.ec.europa.eu/edov2/php/index.php?id=1000

[52] Joint Research Centre (European Commission) *et al.*, *Forest fires in Europe, Middle East and North Africa 2017*. Publications Office of the European Union,

2018. Accessed: Mar. 11, 2024. [Online]. Available: https://data.europa.eu/doi/10.2760/663443

[53] European Commission. Joint Research Centre. Institute for Environment and Sustainability. and European Commission. Directorate General for the Environment., *Forest fires in Europe, Middle East and North Africa 2012.* LU: Publications Office, 2013. Accessed: Mar. 11, 2024. [Online]. Available: https://data.europa.eu/doi/10.2788/58397

[54] M. Turco, M. C. Llasat, J. von Hardenberg, and A. Provenzale, “Impact of climate variability on summer fires in a Mediterranean environment (northeastern Iberian Peninsula),” *Climatic Change*, vol. 116, no. 3, pp. 665–678, Feb. 2013, doi: 10.1007/s10584-012-0505-6.

[55] A. Meyn, P. S. White, C. Buhk, and A. Jentsch, “Environmental drivers of large, infrequent wildfires: the emerging conceptual model,” *Progress in Physical Geography: Earth and Environment*, vol. 31, no. 3, pp. 287–312, Jun. 2007, doi: 10.1177/0309133307079365.

[56] C. Burton, R. A. Betts, C. D. Jones, T. R. Feldpausch, M. Cardoso, and L. O. Anderson, “El Niño Driven Changes in Global Fire 2015/16,” *Front. Earth Sci.*, vol. 8, Jun. 2020, doi: 10.3389/feart.2020.00199.

[57] P. M. Cox *et al.*, “Sensitivity of tropical carbon to climate change constrained by carbon dioxide variability,” *Nature*, vol. 494, no. 7437, pp. 341–344, Feb. 2013, doi: 10.1038/nature11882.

[58] Y. Le Page, J. M. C. Pereira, R. Trigo, C. da Camara, D. Oom, and B. Mota, “Global fire activity patterns (1996–2006) and climatic influence: an analysis using the World Fire Atlas,” *Atmospheric Chemistry and Physics*, vol. 8, no. 7, pp. 1911–1924, Apr. 2008, doi: 10.5194/acp-8-1911-2008.

[59] P. Zhai *et al.*, “The strong El Niño of 2015/16 and its dominant impacts on global and China’s climate,” *J Meteorol Res*, vol. 30, no. 3, pp. 283–297, Jun. 2016, doi: 10.1007/s13351-016-6101-3.

[60] K. Ashok, S. K. Behera, S. A. Rao, H. Weng, and T. Yamagata, “El Niño Modoki and its possible teleconnection,” *Journal of Geophysical Research: Oceans*, vol. 112, no. C11, 2007, doi: 10.1029/2006JC003798.

[61] B. Ayarzagüena, S. Ineson, N. J. Dunstone, M. P. Baldwin, and A. A. Scaife, “Intraseasonal Effects of El Niño–Southern Oscillation on North Atlantic Climate,” *Journal of Climate*, vol. 31, no. 21, pp. 8861–8873, Nov. 2018, doi: 10.1175/JCLI-D-18-0097.1.

[62] “Impact of El Niño–Southern Oscillation on European climate - Brönnimann - 2007 - Reviews of Geophysics - Wiley Online Library.” Accessed: Apr. 22, 2024. [Online]. Available: https://agupubs.onlinelibrary.wiley.com/doi/full/10.1029/2006RG000199

[63] A. Cherchi, H. Annamalai, S. Masina, and A. Navarra, “South Asian Summer Monsoon and the Eastern Mediterranean Climate: The Monsoon–Desert Mechanism in CMIP5 Simulations,” *Journal of Climate*, vol. 27, no. 18, pp. 6877–6903, Sep. 2014, doi: 10.1175/JCLI-D-13-00530.1.

[64] “El Niño and La Niña Years and Intensities.” Accessed: Mar. 14, 2024. [Online]. Available: https://ggweather.com/enso/oni.htm

[65] L. Gudmundsson, F. C. Rego, M. Rocha, and S. I. Seneviratne, “Predicting above normal wildfire activity in southern Europe as a function of meteorological drought,” *Environ. Res. Lett.*, vol. 9, no. 8, p. 084008, Aug. 2014, doi: 10.1088/1748-9326/9/8/084008.

[66] L. Yona, B. Cashore, R. B. Jackson, J. Ometto, and M. A. Bradford, “Refining national greenhouse gas inventories,” *Ambio*, vol. 49, no. 10, pp. 1581–1586, Oct. 2020, doi: 10.1007/s13280-019-01312-9.

[67] A. Cowie, R. Eckard, and S. Eady, “Greenhouse gas accounting for inventory, emissions trading and life cycle assessment in the land-based sector: a review,” *Crop Pasture Sci.*, vol. 63, no. 3, pp. 284–296, May 2012, doi: 10.1071/CP11188.